NUMERICAL STUDY ON THE FLOW AND HEAT TRANSFER OF WATER-BASED Al_2O_3 FORCED PULSATING NANOFLUIDS BASED ON SELF-EXCITED OSCILLATION CHAMBER STRUCTURE

by

Hongmei YUAN [a,b], ***Zhaohui WANG*** [a,b*], ***Quanjie GAO*** [a,b], ***and Ting FU*** [a,b]

[a] Key Laboratory of Metallurgical Equipment and Control Technology of Ministry of Education, Wuhan University of Science and Technology, Wuhan, China
[b] Hubei Key Laboratory of Mechanical Transmission and Manufacturing Engineering, Wuhan University of Science and Technology, Wuhan, China

Original scientific paper
https://doi.org/10.2298/TSCI200906167Y

In this study, the flow and heat transfer characteristics of the forced pulsating Al_2O_3-water nanofluid were numerically studied. The pulsating excitation of the nanofluid is provided by the Helmhertz self-excited oscillating cavity. The large eddy simulation method is used to solve the equation, and the local Nusselt number and heat transfer performance index are used to analyze the heat transfer characteristics of the nanofluid in the self-excited oscillation heat exchange tube. In addition, the effect of different downstream tube diameters on heat transfer enhancement is discussed. The research results show that the existence of the countercurrent vortex can increase the disturbance of the near-wall fluid, thereby improving the mixing degree of the near-wall fluid and the central mainstream. As the countercurrent vortex migrates downstream, pulse enhanced heat transfer is realized. Furthermore, it was also found that when the downstream tube diameter $d_2 = 1.8d_1$, the periodic effect of the local Nusselt number of the wall is the best and the heat transfer performance index has the most stable pulsation effect within a pulsation cycle. But when $d_2 = 2.0d_1$, the change curve of heat transfer performance index in a pulsating period is the highest, the maximum value is 3.95.

Key words*: self-excited oscillation, pulsating nanofluid, enhanced heat transfer, large eddy simulation, countercurrent vortex*

Introduction

In recent years, in order to realize more efficient and energy-saving heat exchange process in heat exchange equipment, passive enhanced heat exchange technology is widely used because it does not require external power. Changing the geometric structure and using nanofluid as a heat transfer medium are common methods to improve heat transfer enhancement. It is reported that the low concentration of nanoparticles greatly improves the heat transfer efficiency of the heat exchange working fluid, thereby significantly increasing the local Nusselt number of heat exchange [1]. In this study, the effects of changing the geometry and using the nanofluids on the flow and heat transfer characteristics are investigated simultaneously. Since the application of forced pulsation nanofluids is in compact heat exchanger equipment, the purpose of this research is to further increase the enhanced heat transfer rate of compact heat exchanger under the premise of energy saving.

[*] Corresponding author, e-mail: zhwang@wust.edu.cn

Some studies have shown that the use of nanofluid as a working medium in the heat exchange tube can increase the heat transfer coefficient, and the heat transfer enhancement increases with the increase of the nanoparticle volume fraction [2-4]. However, Bayat and Nikseresht [5] showed through numerical studies that although nanofluids can increase the convective heat transfer rate, it also require greater pumping power. Similarly, studies have shown that the application of nanofluids in non-straight pipes is more conducive to improving the efficiency of heat transfer enhancement [6-8]. Manca *et al.* [8] also found that the pumping power also increased with the increase of nanoparticles.

Therefore, whether nanofluids are used for heat transfer in straight or non-straight pipes, there is a problem of increased pumping power. On the basis of using nanofluids to enhance the heat transfer rate, in order to reduce the pumping power or keep the pumping power constant, some researchers consider using pulsating nanofluids for heat transfer. Li *et al.* [9] found through numerical research that increasing the pulsation frequency to a certain extent would be more helpful to improve the local and average heat transfer. Sivasankaran and Narrein [10] conducted a numerical analysis on the thermal-hydraulic characteristics of the pulsating water-based Al_2O_3 nanofluid in the porous medium spiral micro-channel radiator. Their research results show that the presence of porous media produces a better heat transfer enhancement effect for sinusoidal velocity inlet conditions compared to steady flow conditions. Naphon and Wiriyasart [11, 12] combine four enhanced heat transfer technologies: pulsating flow, nanofluid, magnetic field, and curved tube (or spiral corrugated tube) to enhance heat transfer. Their experimental results show that thermal boundary-layer disturbance and nanoparticles have significant promoting effects on heat transfer enhancement, and the Nusselt number of pulsating flow is also higher than that of continuous flow. In addition, Zufar *et al.* [13] numerically and experimentally studied the effect of mixed nanofluids on the heat transfer performance of pulsating heat pipes. Experimental results show that, nanofluids can initiate pulses at lower heating power. A review article on the use of nanofluids in heat pipes by Nazari *et al.* [14] pointed out that the use of graphene oxide water nanofluids in pulsating heat pipes can reduce thermal resistance by up to 42%. It can be seen from the aforementioned literature that the pulsating nanofluid is more conducive to heat exchange in the channel. Therefore, it is necessary to study the heat transfer performance of the pulsating nanofluids in heat exchange channels.

At present, researchers have conducted numerical and experimental studies on self-excited oscillation pulse enhanced heat transfer. Wang *et al.* [15] analyzed the feasibility of enhancing heat transfer in the self-excited oscillation shell and tube heat exchanger. The results proved that the application of the self-excited oscillation cavity in the shell and tube heat exchanger cannot only effectively prevent fouling, but also conducive to the structural transformation of the existing shell and tube heat exchanger. Zheng *et al.* [16] conducted an experimental study on the enhancement of pulsation heat transfer. The pulsation of the fluid is generated by a self-excited oscillation cavity. Their research results show that the hydraulic parameters of the fluid and the structure of the self-excited oscillating cavity have a significant effect on the enhancement of fluid pulsation heat transfer. It can be seen that the self-excited oscillation cavity structure not only causes the fluid to pulsate, but also facilitates the structural design according to the different applications of the compact heat exchanger.

Therefore, this paper adopts the large eddy simulation (LES) method to analyze the influence of the Al_2O_3 nanofluid in the flow and heat transfer characteristics of the self-excited oscillation cavity. The flow characteristics of Al_2O_3 nanofluid in the self-excited oscillation heat exchange tube are discussed through the distribution of velocity cloud, temperature cloud, and vorticity cloud. The changes in local Nusselt number and nanofluid heat transfer performance indicators are used to evaluate the heat transfer performance of Al_2O_3 nanofluids in self-excited oscillation heat exchange tubes. In addition, the influence of different downstream pipe diameters on heat transfer enhancement is discussed. The final research results will provide a certain theoretical basis for the optimal design of compact heat exchangers.

Numerical model

Physical model and boundary conditions

Figure 1 shows the schematic diagram of the 2-D geometric structure of the self-oscillating heat exchange tube. The geometric structure of the self-excited oscillation heat exchange tube studied in this paper consists of three parts: the upstream tube, the self-excited oscillation chamber, and the downstream tube. In order to ensure the stability of the inlet flow state of the chamber, the geometry of the upstream channel is consistent with the Helmhertz nozzle inlet structure studied by Liu *et al.* [17]. The upstream pipe-line inlet diameter d_0 = 13 mm, the upstream pipe-line convergence angle is α = 14°, and the upstream pipe-line outlet diameter d_1 = 5.9 mm. At the same time, in order to enable the nanofluid to obtain sufficient pulsation excitation sources, the chamber structure parameters are selected according to the optimal parameter ratio range of Wang *et al.* [18]. The chamber diameter $D = 12d_1$, the chamber length $L = 6d_1$, and the downstream channel diameter d_2 are $1.6d_1$, $1.8d_1$, $2.0d_1$, and $2.2d_1$, respectively. In addition, according to the research of Liu *et al.* [19], it is known that the chamber impingement angle θ = 120° is the best. According to the considered inlet Reynolds number (Re_{in} = 40000), the upstream pipe-line inlet is set as the velocity inlet boundary condition. The downstream pipe-line outlet is set as the pressure outlet boundary condition. The walls of the pipe-line are all set as non-slip boundary conditions and have a uniform and constant temperature of T_w = 400 K. At this time, the upstream pipe-line inlet temperature is set to T_{in} = 298.15K.

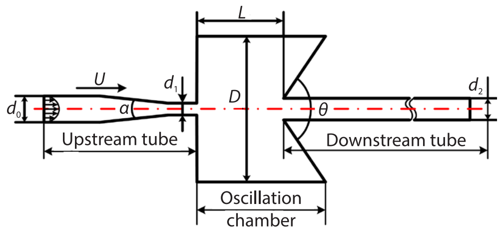

Figure 1. Schematic diagram of the geometric structure of the self-oscillating heat exchange tube

Numerical procedures and governing equations

Numerical procedures

In this study, ANSYS ICEM CFD 17.0 is used to grid the computational domain, and ANSYS FLUENT 17.0 code is used to conduct a 2-D numerical simulation of the self-oscillation heat transfer tube model. The governing equations are solved by the finite volume method. Both the convection and diffusion terms adopt the second-order upwind scheme. In this numerical simulation process, a LES turbulence model based on self-similarity theory is used. This turbulence model is based on the idea of only calculating turbulent large eddies and filtering out small eddies. Subgrid-scale models are used to describe large vortices, and wall-adapting local eddy-viscosity (WALE) model is used to solve eddy viscosity. The SIMPLE algorithm is used to solve the velocity-pressure coupling equation, and the second-order discretization is used to obtain a higher precision numerical solution. Furthermore, in order to achieve a compromise between numerical solution time and accuracy, the maximum residual is set to 10^{-6}.

Governing equations

First make the following assumptions about the working conditions of the computational domain:
– nanoparticles are uniformly distributed in the base fluid and are stable,
– nanofluids are incompressible,
– a constant wall temperature is applied to all walls, and
– the thermophysical properties of the fluid and channel materials are not affected by temperature.

Since the flow boundary has little effect on the small-scale vortices, the filtering method can be used to eliminate the small-scale vortices. After filtering, the incompressible Navier-Stokes equation is written as [20]:
– Continuity equation

$$\frac{\partial \overline{u}_i}{\partial x_i} = 0 \tag{1}$$

– Momentum equation

$$\frac{\partial \overline{u}_i}{\partial t} + \frac{\partial \overline{u}_i \overline{u}_j}{\partial x_j} = \frac{1}{\rho}\left[\frac{\partial}{\partial x_j}\left(\frac{\partial \sigma_{ij}}{\partial x_j}\right) - \frac{\partial \overline{p}}{\partial x_i}\right] - \frac{\partial\left(\overline{u_i u_j} - \overline{u}_i \overline{u}_j\right)}{\partial x_j} \tag{2}$$

where, ρ, u, and p are the density, velocity, and pressure of the working fluid, respectively, σ_{ij} is the stress tensor, defined by molecular viscosity:

$$\sigma_{ij} = \mu\left[\left(\frac{\partial \overline{u}_i}{\partial x_j} + \frac{\partial \overline{u}_j}{\partial x_i}\right) - \frac{2}{3}\frac{\partial \overline{u}_i}{\partial x_i}\delta_{ij}\right] \tag{3}$$

In the WALE model, the eddy viscosity is given:

$$\mu_t = \rho L_s^2 \frac{\left(S_{ij}^d S_{ij}^d\right)^{3/2}}{\left(\overline{S}_{ij}\overline{S}_{ij}\right)^{5/2} + \left(S_{ij}^d S_{ij}^d\right)^{5/4}} \tag{4}$$

where L_{s} and S_{ij}^d in the WALE model are defined, respectively:

$$L_S = \min\left(\kappa d, C_{\mathrm{w}} V^{1/3}\right) \tag{5}$$

$$S_{ij}^d = \frac{1}{2}\left(\overline{g}_{ij}^2 + \overline{g}_{ji}^2\right) - \frac{1}{3}\delta_{ij}\overline{g}_{kk}^2 \overline{g}_{ij} = \frac{\partial \overline{u}_i}{\partial x_j} \tag{6}$$

The value for the WALE constant, C_{w}, is 0.325.

Data reduction

In numerical simulation, the following formulas can be used to calculate Reynolds and Nusselt numbers, pressure drop and friction factor [21]:

$$\mathrm{Re} = \frac{\rho_{\mathrm{nf}} U_{\mathrm{m}} D_{\mathrm{h}}}{\mu_{\mathrm{nf}}} \tag{7}$$

$$\mathrm{Nu} = \frac{h D_{\mathrm{h}}}{\kappa} = \frac{\dot{m} C_p \left(T_{\mathrm{in}} - T_{\mathrm{out}}\right) D_{\mathrm{h}}}{\left(T_{\mathrm{b}} - T_{\mathrm{w}}\right)\kappa} \tag{8}$$

$$f=\frac{2}{\frac{L}{D_\mathrm{h}}}\frac{\Delta p}{\rho_\mathrm{nf}U_\mathrm{m}^2} \tag{9}$$

$$\Delta p=\overline{p}_\mathrm{in}-\overline{p}_\mathrm{out} \tag{10}$$

where T_in and T_out are the inlet and outlet temperatures of the tube, T_b – the bulk mean temperature (the average of the inlet and outlet temperatures), T_w – the tube wall temperature, D_h [m] – the hydraulic diameter, κ – the thermal conduction coefficient, $\dot{m}$ – the mass-flow rate, and C_p – the specific heat at constant pressure.

In order to characterize the heat transfer performance of Al_2O_3 nanofluid in the self-excited oscillation heat exchange tube, the heat transfer performance index (HTPI) is defined. In this study, Al_2O_3 nanofluid is regarded as a single-phase fluid in which nanoparticles and base fluid are uniformly mixed, so the required heat transfer performance standard is derived:

$$HTPI=\frac{E_\mathrm{Nu}}{\left(E_f\right)^{1/3}}=\frac{\frac{\mathrm{Nu}_\mathrm{nf}}{\mathrm{Nu}_\mathrm{bf}}}{\left(\frac{f_\mathrm{nf}}{f_\mathrm{bf}}\right)^{1/3}} \tag{11}$$

where Nu_nf, f_nf, Nu_bf, and f_bf are Nusselt numbers and friction factors of the enhanced (nanofluid-flow inside the self-oscillating tube) and non-enhanced (base fluid-flow inside the straight tube) conditions, respectively. When the value of HTPI is greater than 1, the enhanced heat transfer is high and the pressure drop loss is low. So the index is the bigger the better the parameter.

Thermophysical properties of nanofluid

Correctly specifying the properties of nanofluids is essential to obtain accurate numerical results. This study used a nanofluid with spherical Al_2O_3 nanoparticles with a diameter of 38 nm uniformly distributed in water as the working medium, because Al_2O_3 nanoparticles are more commonly used and relatively inexpensive. Table 1 shows the thermophysical properties of water and Al_2O_3 nanoparticles. In this paper, a single-phase model is used for numerical simulation, and the following equations are used to calculate the thermophysical properties of nanofluids [6]:

– Density

$$\rho_\mathrm{nf}=\sum_{k=1}^{2}\phi_k\rho_k=\left(1-\phi\right)\rho_\mathrm{bf}+\phi\rho_\mathrm{np} \tag{12}$$

– Specific heat

$$\left(\rho C_p\right)_\mathrm{nf}=\left(1-\phi\right)\left(\rho C_p\right)_\mathrm{bf}+\phi\left(\rho C_p\right)_\mathrm{np} \tag{13}$$

– Viscosity

$$\mu_\mathrm{nf}=\frac{\mu_\mathrm{bf}}{\left(1-\phi\right)^{2.5}} \tag{14}$$

– Thermal conductivity

$$\kappa_\mathrm{nf}=\frac{k_\mathrm{np}+2k_\mathrm{bf}-2\phi\left(k_\mathrm{bf}-k_\mathrm{np}\right)}{k_\mathrm{np}+2k_\mathrm{bf}+\phi\left(k_\mathrm{bf}-k_\mathrm{np}\right)}k_\mathrm{bf} \tag{15}$$

Table 1. Thermophysical properties of Al_2O_3 nanoparticles and water [22]

Materials	P [kgm^{-3}]	C_p [Jkg^{-1}K^{-1}]	μ [Pa·s]	κ [Wm^{-1}K^{-1}]
Al_2O_3	3880	773	–	36
Base fluid (water)	998.2	4182	$998 \cdot 10^{-6}$	0.597

Model verification

Grid independence test

When $Re_{in} = 40000$, water is used as the working medium, and the self-excited oscillation heat transfer pipes with structural parameters $D = 12d_1$, $L = 6d_1$, and $d_2 = 1.8d_1$ is tested for grid independence to analyze the grid size Influence of numerical results. Four groups of grids are considered, namely 43395 nodes, 77308 nodes, 172982 nodes, and 354206 nodes. Equation (16) is used to calculate the relative error of Nusselt number under different grids, where M_1 and M_2 represent the average value of Nusselt number under the first and second grids, respectively. Table 2 shows the relative errors of the Nusselt numbers of the previous four grids. Through the comparison of the errors, the grid size of 172982 nodes has been adopted to achieve proper coordination between calculation time and calculation accuracy:

$$e = \left| \frac{M_1 - M_2}{M_1} \right| \times 100\% \tag{16}$$

Table 2. The average Nusselt number for four mesh resolutions

Nodes number	Nu_m	Error [%]
43395	48.749	–
77308	30.283	37.88
172982	27.894	7.89
354206	27.785	0.39

Turbulence model verification

In order to prove the credibility of the numerical results, the numerical model used in this study should be verified. Among the current turbulence models, the direct numerical simulation turbulence model requires higher computer requirements, the LES turbulence model mainly uses different models according to the turbulence structure scale, and the Reynolds average (RANS) turbulence model focuses on the flow.

The field vortex structure can only provide steady flow field results. Since this study needs to consider the vorticity distribution in the turbulence and the computational cost, the LES turbulence model is selected for this simulation. When $Re_{in} = 40000$, the water-based Al_2O_3 nanofluid is used as the working medium to verify the numerical simulation results of the self-excited oscillation heat exchange tube with chamber structure parameters $D = 12d_1$, $L = 6d_1$, and $d_2 = 1.8d_1$. As shown in fig. 2, within one second after the turbulent pulsation reaches a stable state, the relative error range of the average Nusselt number of the current result and Dittus-Boelter empirical formula is 0.11% and 7.8%. The error is less than 10%, indicating that the current numerical simulation results are within the acceptable range of the empirical formula.

Dittus-Boelter's empirical formula [23]:

$$\mathrm{Nu} = 0.023\,\mathrm{Re}^{0.8}\,\mathrm{Pr}^{0.4} \tag{17}$$

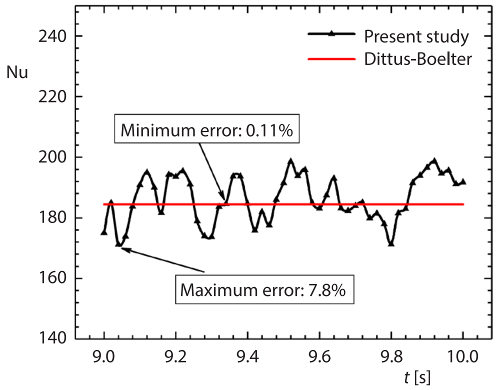

Figure 2. Comparison of Nusselt number under present study with eq. (17)

Results and discussion

In this section, the particle volume fraction, ϕ, of the nanofluids used in the study are all 4%. The flow and heat transfer characteristics of the Al_2O_3-water nanofluid in the self-excited oscillation pulse heat exchange tube and the basic liquid in the straight tube are analyzed by numerical methods.

Distribution of velocity and temperature

Velocity can effectively represent the effect of drag reduction and heat transfer enhancement. Reverse flow in the downstream tube of self-excited oscillating heat exchange tube is considered to be the key to enhanced heat transfer. The velocity distribution of the nanofluid in the self-excited oscillation pulse heat exchange tube within a pulsation period is shown in fig. 3. It is obvious that after the nanofluid-flows through the self-excited oscillation chamber, a pulsating flow will be generated in the downstream pipe. It can also be observed that low speed countercurrent zones and high speed extrusion zones alternately appear on the upper and lower pipe walls, and the low speed countercurrent zone is the key to drag reduction. The velocity near the wall surface in the low velocity countercurrent zone is lower, while the velocity near the wall surface in the high speed extrusion zone will increase. As a result, this increase and decrease in speed will cause the flow velocity in the downstream heat exchange channel to change periodically.

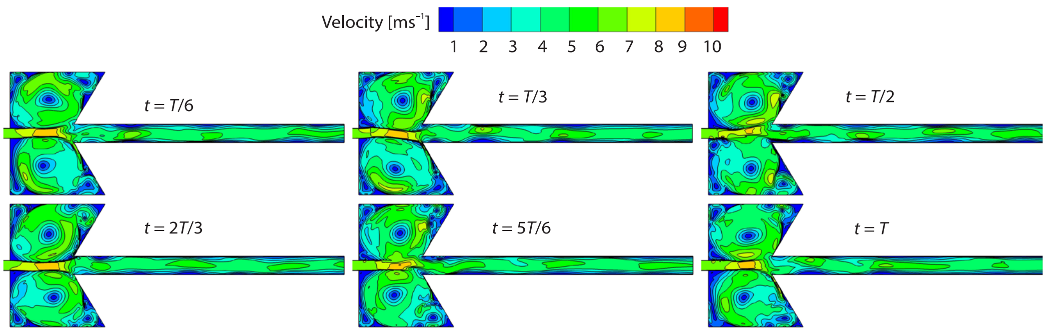

Figure 3. The velocity distribution of the nanofluid in the self-excited oscillating pulse heat exchange tube in a pulsation period

Figure 4 shows the temperature distribution of the working fluid in the self-excited oscillation heat exchange tube in a pulsation period. Compared with fig. 3, it can be seen that the fluid temperature in the low speed countercurrent zone is higher, while the temperature in the high speed extrusion zone is relatively low. According to the isotherm in fig. 4, the high temperature area of the downstream pipe-line is located on both sides of the low speed countercurrent zone, depending on the strength of the countercurrent. And the temperature gradient near the wall reaches the maximum at the countercurrent.

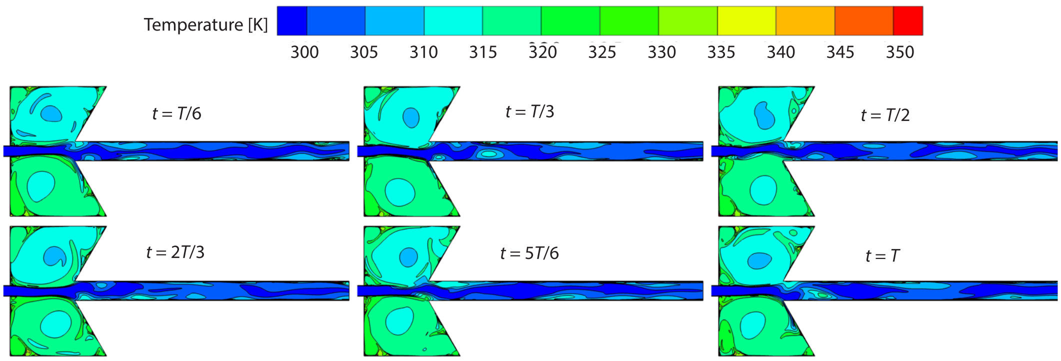

Figure 4. The temperature distribution of the nanofluid in the self-excited oscillating pulse heat exchange tube in a pulsation period

In order to further analyze the periodic changes of the velocity and temperature of the nanofluid in the downstream pipe-line, four reference lines and five reference points are set. Among them, the four monitoring lines are the downstream pipe-line cross-sections, and the distances from the downstream pipe-line inlet are 0 mm, 37.5 mm, 75 mm, and 112.5 mm, respectively, and they are marked as Lines1-4 in sequence. The five reference points are evenly distributed on the reference Line 3. From the upper wall to the lower wall, they are marked as Points 1-5.

Figure 5 shows the velocity and temperature distribution of the downstream pipe-line at the four reference lines. From the figure, it can be found that the low speed re-circulation zone and the high speed extrusion zone alternately appear along the tube wall. In terms of temperature distribution, the temperature gradient near the wall decreases with the axial movement. The thermal boundary-layer at the inlet of the downstream tube is the thinnest, and the closer to the tube outlet, the thicker the thermal boundary-layer. Due to the existence of the countercurrent vortex, the temperature near the wall is significantly higher than that of the central mainstream.

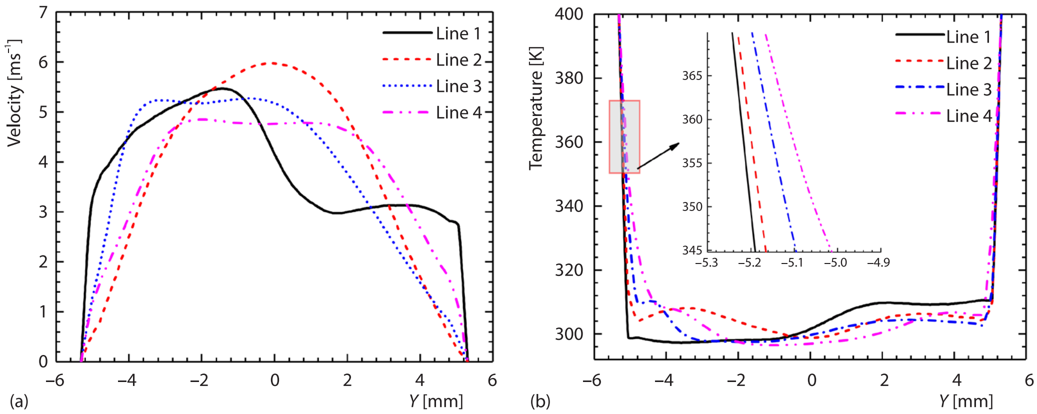

Figure 5. The velocity distribution (a) and temperature distribution (b) of the downstream pipe-line on different reference lines

Figure 6 shows the velocity and temperature changes over time at different reference points. It can be seen from the velocity distribution that Point 1 and Point 5 are located near the wall of the pipe-line, so their velocity is relatively low, and the velocity fluctuations of these two points are opposite. Point 3 is located on the central axis, so its speed is the highest. The velocity fluctuations of Points 2 and 4 present an axisymmetric trend. When analyzing the temperature of each point, it is found that the temperature of Points 1 and 5 is higher and the fluctuation range is larger, while the temperature changes of Points 2-4 are basically the same, and the fluctuation range is smaller. This is because Points 2-4 are located in the central mainstream area, where the flow velocity is faster and the temperature gradient is lower.

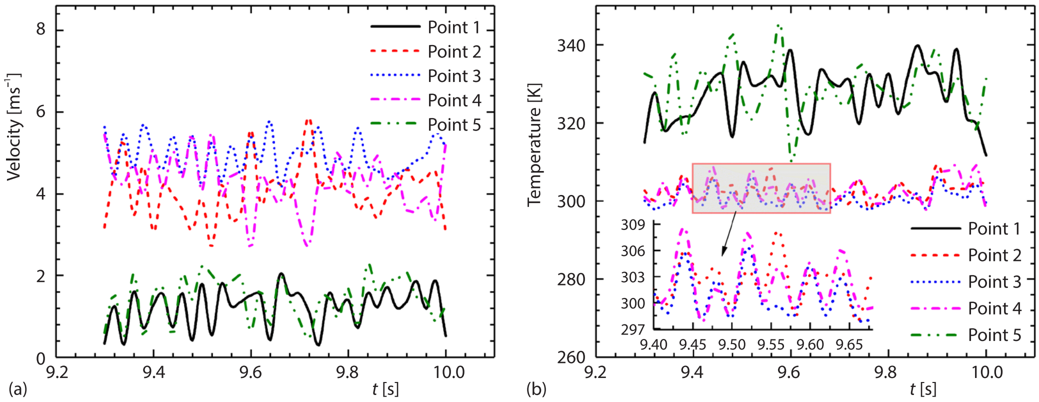

Figure 6. Velocity (a) and temperature (b) at different reference points over time

Vortex distribution in downstream tube

The vorticity can clearly reflect the flow pattern of the nanofluid in the self-excited oscillation pulse heat exchange tube. When the nanofluid reaches the collision wall, a part of the shear flow flows along the collision wall and forms vortices in the chamber. It is the periodic pulses caused by these vortex structures. Other parts of the shear flow flows along the tube wall of the downstream pipe-line. This part of the fluid has a large velocity gradient with the fluid in the central main flow zone, and countercurrent vortexes near the wall of the downstream tube.

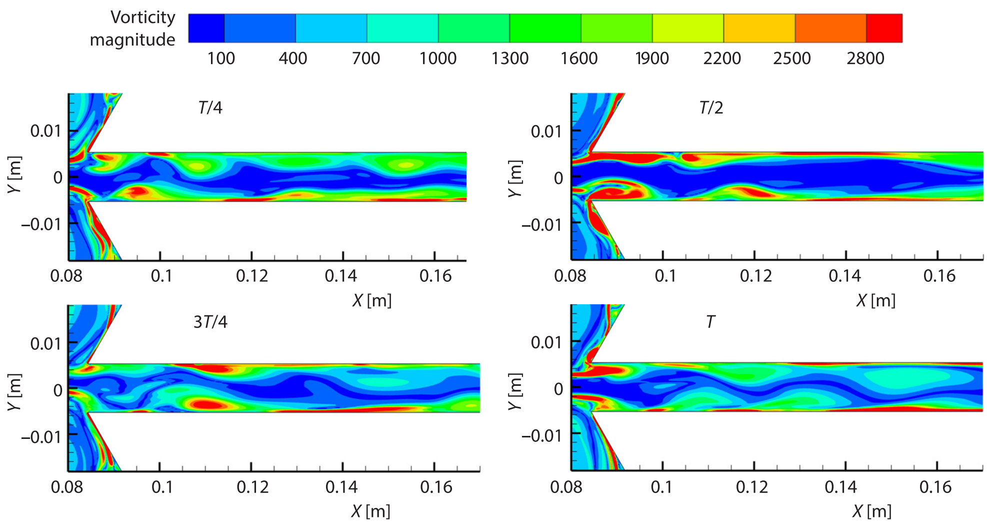

Figure 7. The vorticity distribution of the downstream pipe-line in a pulsation period

The vorticity distribution in the downstream tube is shown in fig. 7. It can be observed that at $t = T/4$, the shear flow is about to reach the collision wall, and the shear flow of the previous cycle has gradually dissipated in the downstream pipe-line. At $t = T/2$, the shear flow has reached the collision wall and is divided into two parts by the collision sharp corner, forming a countercurrent vortex near the downstream pipe inlet. At $t = 3T/4$, the countercurrent vortex falls off the chamber and migrates downstream, near the wall near $x = 0.11$ m, the disturbance is the largest. At $t = T$, the countercurrent vortex in the downstream pipe-line has gradually dissipated, and the shear flow in the chamber is preparing for the next collision and separation. In addition, it can be seen from the figure that both sides of the counter-current vortex near the wall of the downstream tube show lower vorticity, which is caused by the high speed extrusion micelles between two adjacent counter-current vortices. As the countercurrent vortex migrates downstream, the flow velocity near the wall of the tube exhibits periodic fluctuations, which indicates that the existence of the countercurrent vortex increases the volatility of the disturbance near the wall, thereby enhancing the mixing of hot and cold fluids in the tube.

Heat transfer changes in downstream tubes

Wall shear stress and Nusselt number

The greater the wall shear stress, the greater the flow velocity of the fluid near the wall and the stronger the disturbance. The left image of fig. 8 compares the wall shear stress curve of self-excited oscillation heat exchange tubes with different downstream tube diameters and smooth tubes. It can be seen from the figure that in a smooth round tube without a self-excited oscillation cavity structure, the wall shear stress decreases linearly along the wall and changes little. In the self-excited oscillation heat exchange tube, the wall shear stress presents a periodic change trend due to the collision and separation of the shear flow. Among them, when $d_2/d_1 = 1.6$ and 2.0, the wall shear stress has a higher pulsation amplitude, but its fluctuation stability is relatively poor; when $d_2/d_1 = 1.8$ and 2.2, the fluctuating amplitude of wall shear stress is smaller than the first two cases, and its periodicity is relatively stable. The best periodic wall shear stress is obtained when $d_2/d_1 = 2.2$. In general, all the self-excited oscillation heat exchange tubes studied are higher than the wall shear stress of smooth round tubes, and when $d_2/d_1 = 1.8$ and 2.2, the wall shear stress is higher and the periodicity is more stable, so the self-excited oscillation heat exchange tubes with $d_2/d_1 = 1.8$ and 2.2 have larger disturbances near the wall.

The larger the Nusselt number, the better the heat transfer enhancement effect. The right image of fig. 8 shows the variation of the Nusselt number of the self-excited oscillation heat exchange tube and smooth tube with different downstream pipe diameters. It can be observed that the local Nusselt number of the smooth circular tube wall has the same changing trend as the wall shear stress. In the self-excited oscillating heat exchange tube, the local Nusselt number on the wall also shows a periodic change trend. Moreover, the local Nusselt number of the wall of the self-excited oscillation tube is generally better than that of the smooth round tube, indicating that the enhanced heat transfer effect of the nanofluid in the self-excited oscillation tube is significantly better than that of the base fluid in the smooth round tube. It is also found that when $d_2/d_1 = 2.0$, the fluctuation peak of the Nusselt number of the wall gradually decreases along the wall, indicating that the pulsation at this time is not continuous. When $d_2/d_1 = 1.6$, 1.8, and 2.2, the periodic pulsation effect of the wall Nusselt number is better, so the downstream pipe diameter at this time is more conducive to the enhancement of heat transfer.

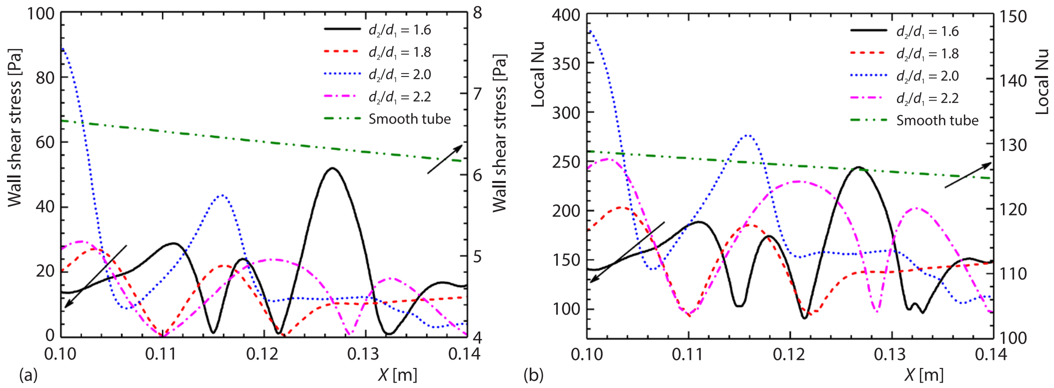

Figure 8. Wall shear stress (a) and local Nusselt number (b) of the self-oscillation heat exchange tube and smooth tube in the downstream pipe-line

Heat transfer performance index

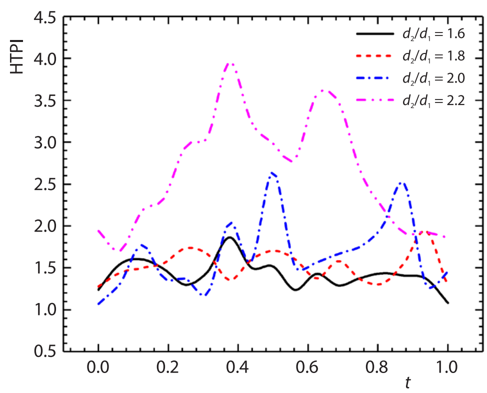

Figure 9. The HTPI varies with different downstream pipe diameters during a pulsating period

Figure 9 shows the change of HTPI of self-excited oscillation heat exchange tubes with different downstream pipe diameters in a pulsation period. It can be seen that HTPI is greater than 1 in all studies, indicating that the existence of the self-oscillation structure can effectively improve the heat transfer performance. Among them, when d_2/d_1 = 1.6, 1.8, 2.0, and 2.2, the maximum value of HTPI in a pulsating period is 1.86, 1.94, 2.64, and 3.95, respectively. In general, when d_2/d_1 = 1.6, 1.8, HTPI fluctuates more stably within a pulsating cycle; when d_2/d_1 = 2.0, the periodicity of HTPI is the worst, indicating that the enhanced heat transfer is unstable. When d_2/d_1 = 2.2, the periodicity of HTPI fluctuation is relatively stable and the value is relatively high. The maximum HTPI value is 3.95, which shows that the heat transfer enhancement effect is the best at this time.

Conclusions

In this study, the flow and heat transfer of water-based Al_2O_3 nanofluids in a heat exchange pipe with a self-excited oscillation cavity structure were studied by LES. This numerical results obtained are compared with base fluid in the straight pipe. In addition, the influence of the dimensionless structure parameter d_2/d_1 of the chamber on the heat transfer performance at different values is also studied. The main conclusions of this study are as folows.

- In the downstream pipe-line, the flow near the wall can be divided into two areas: low speed countercurrent and high speed extrusion. The temperature in the low speed countercurrent zone is relatively high, while the temperature in the high speed extrusion zone is relatively low. The low speed re-circulation zone and the high speed extrusion zone alternately appear along the wall. Moreover, the shear flow generated by the self-excited oscillation cavity is the key to the formation of countercurrent vortices in the downstream pipe-line. There is a large velocity gradient between the shear flow near the wall of the downstream pipe-line and the fluid in the central mainstream zone, which causes the formation of a countercurrent vortex near the near-wall of the downstream pipe-line. As the countercurrent vortex migrates downstream, periodic pulsating heat transfer is realized.

- In addition, through the analysis of wall shear stress and Nusselt number, when d_2/d_1 = 1.8 and 2.2, the disturbance near the wall of the downstream pipe-line is the largest and the Nusselt number periodicity is more obvious. The HTPI fluctuates most stable when d_2/d_1 = 1.8, and the maximum value reaches 3.95 when d_2/d_1= 2.2. Therefore, these two structures are most conducive to the enhanced heat transfer of nanofluids.

Acknowledgment

This work was supported by the National Natural Science Foundation of China (Grant No. 51875419).

Nomenclature

C_p – specific heat, [Jkg^{-1}K–1]
d_0 – diameter of upstream tube inlet, [m]
d_1 – diameter of upstream tube outlet, [m]
d_2 – diameter of downstream tube, [m]
d_2/d_1 – dimensionless parameter, [–]
D – diameter of chamber, [m]
D_h – hydraulic diameter, [m]
Δp – pressure drop, [Pa]
f – friction factor, [–]
h – heat transfer coefficient, [Wm^{-2}K–1]
L – length of chamber, [m]
Nu – Nusselt number (= hD_h/κ), [–]
Pr – Prandtl number (= $C_p\mu/\kappa$), [–]
Re – Reynolds number (= $\rho UD_h/\mu$), [–]
T – temperature, [K]
U – velocity, [ms^{-1}]

Greek symbols

α – convergence angle of upstream tube, [°]
θ – impingement angle of chamber, [°]
κ – thermal conductivity, [Wm^{-1}K^{-1}]
μ – dynamic viscosity, [Nsm^{-2}]
ρ – density, [kgm^{-3}]
ϕ – volume friction of nanoparticles, [%]

Subscirpts

b – bulk
bf – base fluid
in – inlet
m – mean
nf – nanofluid
np – nanoparticle
out – outlet
w – wall

References

[1] Keblinski, P., *et al.*, Mechanisms of Heat Flow in Suspensions of Nanosized Particles (Nanofluids), *International Journal of Heat and Mass Transfer*, *45* (2002), 4, pp. 855-863
[2] Santra, A. K., *et al.*, Study of Heat Transfer Due to Laminar Flow of Copper-Water Nanofluid through Two Isothermally Heated Parallel Plates, *International Journal of Thermal Sciences*, *48* (2009), 2, pp. 391-400
[3] Ahmadi, A. A., *et al.*, Numerical Study of Flow and Heat Transfer of Water-Al_2O_3 Nanofluid Inside a Channel with an Inner Cylinder Using Eulerian-Lagrangian Approach, *Journal of Thermal Analysis and Calorimetry*, *132* (2017), 1, pp. 651-665
[4] Bianco, V., *et al.*, Numerical Investigation on Nanofluids Turbulent Convection Heat Transfer Inside a Circular Tube, *International Journal of Thermal Sciences*, *50* (2011), 3, pp. 341-349
[5] Bayat, J., Nikseresht, A. H., Thermal Performance and Pressure Drop Analysis of Nanofluids in Turbulent Forced Convective Flows, *International Journal of Thermal Sciences*, *60* (2012), Oct., pp. 236-243
[6] Nazari, S., Toghraie, D., Numerical Simulation of Heat Transfer and Fluid-Flow of Water-CuO Nanofluid in a Sinusoidal Channel with a Porous Medium, *Physica E: Low-dimensional Systems and Nanostructures*, *87* (2017), Mar., pp. 134-140
[7] Saffarian, M. R., *et al.*, Heat Transfer Enhancement in a Flat Plate Solar Collector with Different Flow Path Shapes Using Nanofluid, *Renewable Energy*, *146* (2020), Feb., pp. 2316-2329
[8] Manca, O., *et al.*, A Numerical Study of Nanofluid Forced Convection in Ribbed Channels, *Applied Thermal Engineering*, *37* (2012), May, pp. 280-292

[9] Li, P., *et al.*, Mechanism Analysis of Heat Transfer and Flow Structure of Periodic Pulsating Nanofluids Slot-Jet Impingement with Different Waveforms, *Applied Thermal Engineering*, *152* (2019), Apr., pp. 937-945

[10] Sivasankaran, S., Narrein, K., Numerical Investigation of Two-Phase Laminar Pulsating Nanofluid-Flow in Helical Micro-Channel Filled with a Porous Medium, *International Communications in Heat and Mass Transfer*, *75* (2016), July, pp. 86-91

[11] Naphon, P., Wiriyasart, S., Pulsating Flow and Magnetic Field Effects on the Convective Heat Transfer of TiO_2-Water Nanofluids in Helically Corrugated Tube, *International Journal of Heat and Mass Transfer*, *125* (2018), Oct., pp. 1054-1060

[12] Naphon, P., Wiriyasart, S., Pulsating TiO_2-Water Nanofluids Flow and Heat Transfer in the Spirally Coiled Tubes with Different Magnetic Field Directions, *International Journal of Heat and Mass Transfer*, *115* (2017), Dec., pp. 537-543

[13] Zufar, M., *et al.*, Numerical and Experimental Investigations of Hybrid Nanofluids on Pulsating Heat Pipe Performance, *International Journal of Heat and Mass Transfer*, *146* (2020), Jan., 118887

[14] Nazari, A. M., *et al.*, A Review on Using Nanofluids in Heat Pipes, *Journal of Thermal Analysis and Calorimetry*, *137* (2019), 6, pp. 1847-1855

[15] Wang, F. S., *et al.*, A Feasibility Analysis of Applying Self-Excited Oscillation Shell and Tube Heat Exchanger for Heat Transfer Enhancement (in Chinese), *Industrial Heating*, *36* (2007), 3, pp. 56-58

[16] Zheng, J., *et al.*, Experimental Study of Heat Transfer Enhancement with Pulsating Flow (in Chinese), *Heat Transfer Asian Research*, *33* (2004), 5, pp. 279-286

[17] Liu, W. C., *et al.*, Self-Sustained Oscillation and Cavitation Characteristics of a Jet in a Helmholtz Resonator, *International Journal of Heat and Fluid-flow*, *68* (2017), Dec., pp. 158-172

[18] Wang, L. Q., *et al.*, Experimental Study on Structural Parameters Optimized Design of the Self-Excited Oscillation Pulsed Jet Nozzle (in Chinese), *Journal of engineering thermophysics*, *25* (2004), 6, pp. 956-958

[19] Liu, W. C., *et al.*, Experimental and Theoretical Analysis on Chamber Pressure of a Self-Resonating Cavitation Waterjet, *Ocean Engineering*, *151* (2018), Mar., pp. 33-45

[20] Fang, Z. L., *et al.*, Large Eddy Simulation of Self-Excited Oscillation Inside Helmholtz Oscillator, *International Journal of Multi-phase Flow*, *126* (2020), Feb., 103253

[21] Khoshvaght-Aliabadi, M., Influence of Different Design Parameters and Al_2O_3-Water Nanofluid-Flow on Heat Transfer and Flow Characteristics of Sinusoidal-Corrugated Channels, *Energy Conversion and Management*, *88* (2014), Dec., pp. 96-105

[22] Khoshvaght-Aliabadi, M., *et al.*, The Al_2O_3-Water Nanofluid Inside Wavy Mini-Channel with Different Cross-Sections, *Journal of the Taiwan Institute of Chemical Engineers*, *58* (2016), Jan., pp. 8-18

[23] Yarmand, H., *et al.*, Convective Heat Transfer Enhancement with Graphene Nanoplatelet/Platinum Hybrid Nanofluid, *International Communications in Heat and Mass Transfer*, *88* (2017), Nov., pp. 120-125

Paper submitted: September 6, 2020
Paper revised: March 5, 2021
Paper accepted: March 11, 2021